

## **Quantitative Evaluation of Light-to-Heat Conversion and Singlet Oxygen Generation Efficiencies on Ligand Protected Gold Nanoclusters upon Near-infrared Excitation**

Lisa Verheyde, Hao Yuan, Isabelle Russier-Antoine, Stéphane Joly, Pierre-François Brevet, Rodolphe Antoine\* and Sangita Kundu\*

Institut Lumière Matière, University of Lyon, Université Claude Bernard Lyon 1, CNRS, Lyon

F-69622, France. Email: [rodolphe.antoine@univ-lyon1.fr](mailto:rodolphe.antoine@univ-lyon1.fr); [sangita.kundu@univ-lyon1.fr](mailto:sangita.kundu@univ-lyon1.fr)

**1.1. Mass spectrometry (MS).** MS measurements were performed by variable temperature-nano-electrospray ionization on a commercial quadrupole time-of-flight mass spectrometry system (micro-qTOF, Bruker-Daltonics, Bremen, Germany, mass resolution 10,000). The thermalized nano-Electrospray ionization (ESI) source (homemade) maintained a temperature at 21 °C. Solutions were prepared in water at a concentration of approximately 25  $\mu\text{M}$  and directly sprayed using the original electrospray source of the instrument.<sup>1</sup> The samples were analyzed in negative ion mode; each data point was the summation of spectra over 5 min.

**1.2. Transmission electron microscopy (TEM).** Morphological studies were performed using transmission electron microscopy (TEM, JEOL-JEM-F2100) at an operating voltage of 200 kV. TEM samples were prepared by drop-casting solutions onto carbon-coated gold grids.

**1.3. Optical spectroscopy.** For UV–vis absorption spectra, the NC solutions were diluted with water to a final concentration of 10  $\mu\text{M}$  and then were measured on an Avantes AvaSpec-2048 spectrophotometer with an AvaLight DH-S deuterium lamp with water as reference. All measurements were conducted with a 1 cm quartz cuvette.

**1.4. Two-photon absorption experiments.** The light source for the present two photon absorption and emission experiments was a mode locked femtosecond Ti:sapphire laser delivering at the fundamental wavelength of 808 nm pulses with a duration of about 140 femtoseconds at a repetition rate of 80 MHz. The beam was gently focused by a 5 cm focal length lens to a waist of 10  $\mu\text{m}$  and sent in transmission into a 0.5 cm path length spectrophotometric cuvette. The

transmitted light was detected with a large aperture photodiode. The incident power was controlled with a half-wave plate and a polarizing cube. The sample absorption was then determined as a function of the incident power. Nonlinear absorption was probed using the P-scan (or Power-scan) technique during which the incident power is directly varied and the induced changes in the sample transmission are measured, as detailed in our previous works.<sup>2</sup>

### 1.5. Photothermal experiment under CW laser excitation.

The photothermal effect of Au NCs was evaluated by using a thermal infrared imager (FLIR C5) to record the temperature change of the same at different time intervals under 808 nm LED diode laser irradiation (Laser 2000). Briefly, a solution of Au NCs at 1 mg/mL was irradiated by an 808 nm laser (2 W power) until the temperature reached a stable temperature (20 min), and then the laser was removed. The heated solution was monitored and allowed to cool to its starting temperature. To further evaluate the photothermal conversion efficiency ( $\eta$ ) of Au NCs, 2 mL of the same was added into a standard quartz cell and given continuous 808 nm laser exposure for 20 min. Then, the laser was removed immediately, and the solution was allowed to cool naturally to its starting temperature. As a control, 1 mL of DI water was used in the same process to obtain the heat absorbed by the quartz cell and water ( $Q_{Dis}$ ). The thermal infrared imager was used to record the temperature change of Au NCs solution and DI water during the whole process. The value of  $\eta$  was calculated according to equations reported by Roper et al.<sup>3</sup>

The photothermal conversion efficiency ( $\eta$ ) was calculated according to the following equations:

$$\eta_{cw} = \frac{[hS \times (T_{max} - T_{surr}) - Q_{Dis}]}{[I \times (1 - 10^{-A_{808}})]} \times 100 \quad (1)$$

In order to determine  $hS$ , a dimensionless parameter  $\theta$  is introduced as followed:

$$\theta = \frac{(T - T_{surr})}{(T_{max} - T_{surr})} \quad (2)$$

A sample system time constant can be calculated as Eq.3.

$$t = \tau_s \times (-\ln\theta) \quad (3)$$

$$hS = \frac{m_{DCD}}{\tau_s} \quad (4)$$

where  $h$  is the heat transfer coefficient,  $S$  is the surface area of the container, and the value of  $hS$  is obtained from the Eq.4. The maximum steady temperature ( $T_{max}$ ) of the solution of the Au NCs was varied for different NCs and environmental temperature ( $T_{Surr}$ ) was 21 °C. The laser power  $I$  is 2 W. The absorbance of the Au NCs at 808 nm was taken into account.  $Q_{Dis}$  expresses heat dissipated from the light absorbed by the solvent and container.

In addition,  $m$  is 2 g and  $C$  is 4.2 J/g °C.  $Q_{Dis}$  expresses heat dissipated from the light absorbed by the quartz sample cell itself, and it was measured independently to be 0.19 mW using a quartz cuvette cell containing pure water.

### 1.6. Photothermal experiment under femtosecond laser excitation.

The photothermal effect of Au NCs was evaluated by using a thermal infrared imager (FLIR C5) to record the temperature change of the same at different time intervals under mode locked femtosecond Ti:sapphire laser delivering at the fundamental wavelength of 808 nm pulses with a duration of about 140 femtoseconds at a repetition rate of 80 MHz. Briefly, a solution of Au NCs at 1 mg/mL was irradiated by an 808 nm laser (1.9 W power) until the temperature reached a stable temperature (15 min), and then the laser was removed immediately. The heated solution was monitored and allowed to cool to its starting temperature. The value of  $\eta$  was calculated according to equations by modified Roper model accounting for nonlinear optical effects for photon absorption.

#### Modified Roper's Model

A continuum energy balance on NP suspension irradiated by a laser gives (Eq.5) :

$$\sum mc_p \frac{dT}{dt} = Q_L + Q_0 - Q_{ext} \quad (5)$$

which describes the heating of the nanoparticle solution by laser irradiation.

$\sum mc_p$  is a sum of products of mass and heat capacities of all system components,  $\frac{dT}{dt}$  is the rate of temperature increase,  $Q_{ext}$  is external heat flux,  $Q_0 + Q_L$  is heat produced by converting the absorbed light into heat, by either solvent ( $Q_0$ ) or by the nanoparticles ( $Q_L$ ). The  $Q_L$  is determined by the following equation:

$$Q_L = I(1 - 10^{-A_\lambda}) \eta_Q \quad (6)$$

where  $I$  is a laser power,  $\eta_Q$  represents the light-to-heat conversion efficiency,  $A_\lambda$  is the absorbance at irradiation wavelength  $\lambda$  and is measured experimentally using Lambert–Beer’s law.

When ultrashort pulses of the excitation are applied,  $Q_L$  should be expanded to take into account the average pumping power based on the energy, pulse duration, and pulse frequencies. Starting from the attenuation of light in matter at the depth  $z$  due to one- and two-photon absorption, we solve the following equation for the intensity  $I$ ,

$$\frac{dI}{dz} = -\alpha I - \beta I^2 \quad (7)$$

where  $\alpha$  is the one- and  $\beta$  the two-photon absorption coefficient.

In the case of linear one-photon absorption, we set  $\beta = 0$ , which results in Lambert-Beer’s Law. In the case of pure 2-photon absorption, we set  $\alpha = 0$

If  $I_0$  is the incident laser intensity (W/cm<sup>2</sup>), the solutions of Eq. (7) are

$$I = I_0 e^{-\alpha z} \quad \text{for } \beta = 0 \quad (8a)$$

$$I = \frac{I_0}{1 + \beta I_0 z} \quad \text{for } \alpha = 0 \quad (8b)$$

If both  $\beta$  and  $\alpha$  cannot be neglected at the wavelength considered, the solution of Eq. (12) is:

$$I = \frac{I_0}{1 + \frac{\beta}{\alpha} I_0 z (1 - e^{-\alpha z})} e^{-\alpha z} \quad (8c)$$

with  $\alpha = \frac{A_\lambda}{z} \ln 10$  and  $\beta$  is the 2PA coefficient, characteristic macroscopic parameter of the material and is closely related to the 2PA cross section (2PA) by

$$\sigma(2PA) = \frac{E}{N_0} = \frac{1000 hv \beta}{N_A C} \quad (9)$$

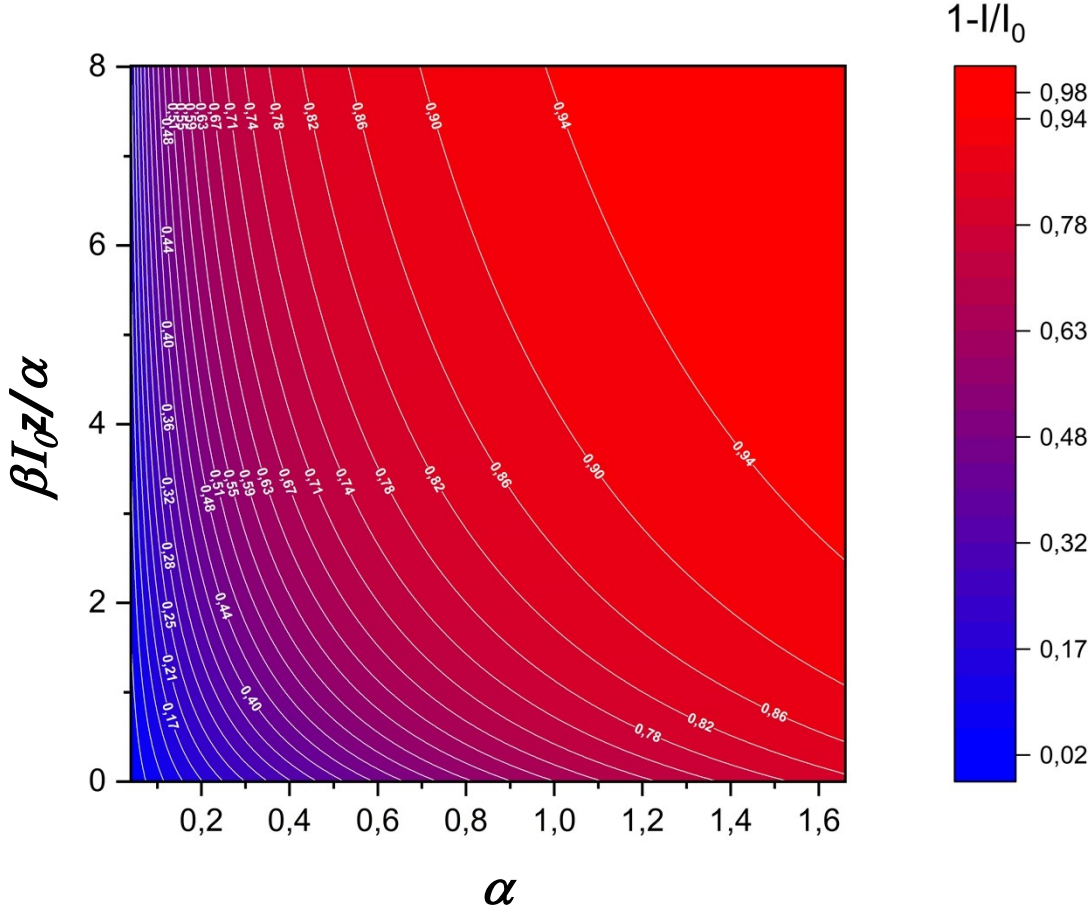
where  $N_0$  is the molecular density of the compound (number of molecules per unit volume) and  $E$  is the photon energy,  $hv$  is the energy of the photons,  $N_A$  is Avogadro's number and  $C$  is the molecular concentration. The molecular 2PA cross section is quoted in the units of Göppert-Mayer GM (where  $1 \text{ GM} = 10^{-50} \text{ cm}^4 \text{ s photon}^{-1}$ ) and  $\beta$  in  $\text{cm.W}^{-1}$ .

Then

$$Q_L = P_0 \left(1 - \frac{I}{I_0}\right) \eta_Q \quad (10)$$

with  $\left(1 - \frac{I}{I_0}\right)$  given by Eq. 8(a-c) depending on the photon regime and  $P_0$  is the average laser power of the laser. The evolution of  $\left(1 - \frac{I}{I_0}\right)$  as a function of  $\beta$  and  $\alpha$  is given by the following Map S1,

evidencing the balance between one- and two-photon absorption in the  $(1 - \frac{I}{I_0})$  correction.



**Map S1.** Evolution of  $(1 - \frac{I}{I_0})$  using Eq.8c as a function of  $\alpha$ , and  $\beta I_0 z / \alpha$ .

Then the photothermal conversion efficiency ( $\eta$ ) is calculated according to the following equation:

$$\eta_{fs} = [hS \times (T_{max} - T_{surr}) - Q_{Dis}] / Q_L \quad (11)$$

### 1.7. Singlet oxygen generation experiment.

The singlet oxygen generation efficiency was measured by an indirect method with the  $^1O_2$  sensor of 1,3-diphenylisobenzofuran (DPBF).<sup>4</sup> Absorption spectra of DPBF was monitored under the irradiation by a absorption spectrometer. For one-photon  $^1O_2$  generation, 808 nm CW laser (Laser 2000) was used with an output power of 1 W and a beam diameter of 8 mm. For two-photon  $^1O_2$

generation, mode locked femtosecond Ti:sapphire laser was used with 808 nm pulses (Duration: 140 femtoseconds, repetition rate of 80 MHz) at average output power of 1 W. A typical solution used in the experiment contained nanoclusters/nanoparticles/dyes and DPBF with a concentration of  $0.3425 \times 10^{-6}$  M and  $1.53 \times 10^{-5}$  M, respectively. All solutions were prepared in ethanol. The mixture solution with ethanol-water solvent (50/50 in volume ratio) was used. The samples were loaded in quartz cuvettes (1cm light path length) and the absorbance was recorded with irradiation for different time.

### **singlet oxygen generation rate.**

The concentration of DPBF was calculated from the intensity of absorption peak at 412 nm according to Beer–Lambert law. The rate of  $^1\text{O}_2$  generation was obtained by the initial DPBF concentration change over time by a function:

$$\text{rate of } ^1\text{O}_2 \text{ generation} = \frac{c[\text{DPBF}]_{0 \text{ min}} - c[\text{DPBF}]_{5 \text{ min}}}{\Delta t} / c[\text{NCs}] \quad (12)$$

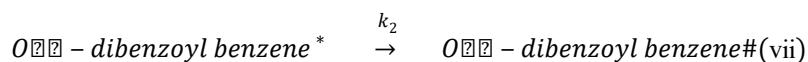
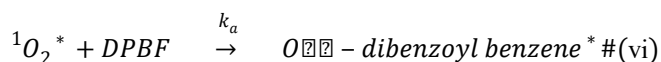
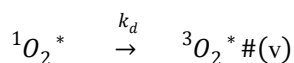
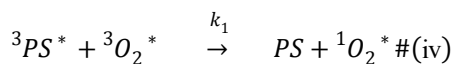
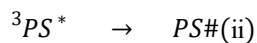
$c[\text{DPBF}]_{0 \text{ min}}$  and  $c[\text{DPBF}]_{5 \text{ min}}$  represent the concentration of DPBF at 0 min and 5 min under irradiation,  $\Delta t$  respectively. represents the time under irradiation (5 mins), and  $c[\text{NCs}] = 1.37 \times 10^{-6}$  M. The photoluminescence lifetime was calculated by two-exponential fitting in the decay curve. The uncertainty was evaluated by measuring 3 times repeatedly.

### **singlet oxygen generation quantum yield.**

According to Marin et al.'s and Damera et al.'s work <sup>5,6</sup>, the singlet oxygen generation rate was calculated from the chemical quenching of DPBF.

The mechanism for generation of singlet oxygen, and the interaction between singlet oxygen and DPBF with PS the photosensitizer is given by:





The efficiency of DPBF oxidation was calculated to Eqn (12):

$$\phi_{DPBF} = \frac{-\frac{\partial[DPBF]}{\partial t}}{I_a} = \phi_{\Delta} \left( \frac{k_a[DPBF]}{k_a[DPBF] + k_d} \right) \#(13)$$

Where  $I_a$  is the rate of light absorption by PS,  $k_a$  is the rate constant for the reaction between singlet oxygen and DPBF,  $k_d$  is the rate constant for the decay of singlet oxygen,  $\phi_{\Delta}$  is the singlet oxygen quantum yield.

Eqn (13) can be integrated into eqn (14):

$$\left[ \Delta[DPBF] + \frac{k_d}{k_a} \ln \frac{[DPBF]_t}{[DPBF]_0} \right] = -I_a \phi_{\Delta} t \#(14)$$

By a textbook, for the DPBF- ${}^1O_2$  reaction, in ethanol,  $k_d = 8.3 \times 10^4 M^{-1} s^{-1}$ ,  $k_a = 1.28 \times 10^9 M^{-1} s^{-1}$ .<sup>7</sup>

When the left-hand side of eqn (2) was plotted against time (as shown in Figure S5 below), the slope of this line is equal to  $-I_a \phi_{\Delta}$ .<sup>8</sup>

$I_a$  in eqn (18) represents moles of photons absorbed per unit time and volume, which can be calculated by eqn (19):

$$I_a = \left(1 - \frac{I}{I_0}\right) \left(\frac{P_0 \lambda_{ex}}{hc N_A V}\right) \#(15)$$

$\lambda_{ex}$  is the absorbance of the photosensitizer at the excitation wavelength,  $h$  is the Planck constant,  $c$  is the light speed  $N_A$  is Avogadro's number and  $V$  is the reaction volume (2 mL). For both cw and pulsed laser excitation, a power  $P_0$  of 1 W power was used.

with  $\left(1 - \frac{I}{I_0}\right)$  given by Eq. 8(a-c) depending on the photon regime.

**1.8. Cell viability assay.** For cell viability, MTT assay was performed (BIOTIUM, MTT Assay kit). For MTT assay, about 10000 cells were seeded in the wells of a 96-well plate. Cells were allowed to adhere and grow in the wells for 24 h after which the NCs were added in different concentrations of 10, 20, 50, 100 and 200  $\mu\text{g/mL}$ . Dilutions of the clusters were prepared in DMEM culture medium by dissolving the powder of the NCs. It should be noted that the highest concentration of 200  $\mu\text{g/mL}$  corresponds to 26  $\mu\text{M}$  Au<sub>25</sub>pMBA<sub>18</sub> (128  $\mu\text{g}$  of Au in 1 mL), 7.4  $\mu\text{M}$  Au<sub>102</sub>pMBA<sub>44</sub> (150  $\mu\text{g}$  of Au in 1 mL) and 3.6  $\mu\text{M}$  Au<sub>~288</sub>(pMBA)<sub>~92</sub> (160  $\mu\text{g}$  of Au in 1 mL). After addition of the NCs, plates were incubated at 37 °C for 48h. After incubation, medium was removed from the wells, 2 washes with PBS IX were done and MTT reactive diluted in culture medium at a final concentration of 0.5 mg/mL was added to the wells. The cells were allowed to incubate in dark in the incubator at 37°C for 1h and visualized under the microscope for formazan crystals. The media containing MTT was discarded and the formazan filled cells were dissolved in 100  $\mu\text{L}$  of DMSO. Formazan was allowed to solubilise for 15 min after which the absorbance was measured in a UV-visible spectrophotometer multiwell plate reader (VICTOR Nivo, Perkin Elmer) at 570 nm and at 630 nm for the background. Only complete DMEM medium were added in positive control wells. The cell viability was measured using the formula:

$$\text{Cell Viability} = \frac{S - B_S}{PC - B_{PC}} \quad (16)$$

where S= test sample, B= background, PC= positive control.

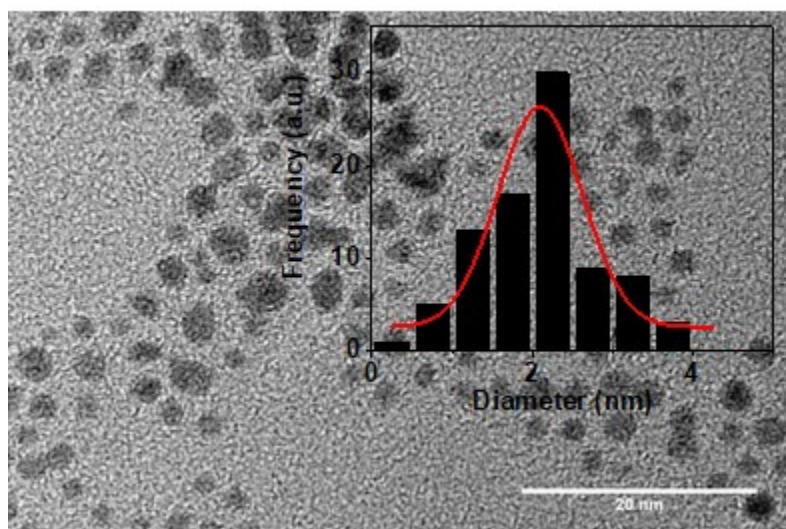


**Figure S1.** TEM images of  $\text{Au}_{\sim 288}(\text{pMBA})_{\sim 92}$  NCs. The inset shows the corresponding size distribution histogram of the same.

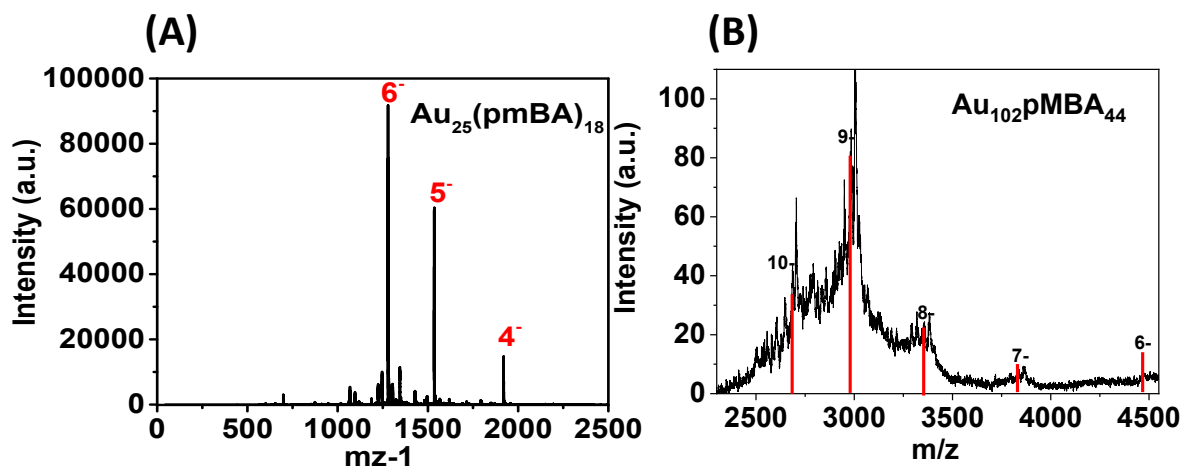


**Figure S2.** ESI mass spectra of (A)  $\text{Au}_{25}(\text{pMBA})_{18}$  and (B)  $\text{Au}_{102}(\text{pMBA})_{44}$  NCs. The red bars in panel B indicate calculated peak positions for  $[\text{Au}_{102}(\text{p-MBA})_{44} - n\text{H}^+]^{n-}$ .

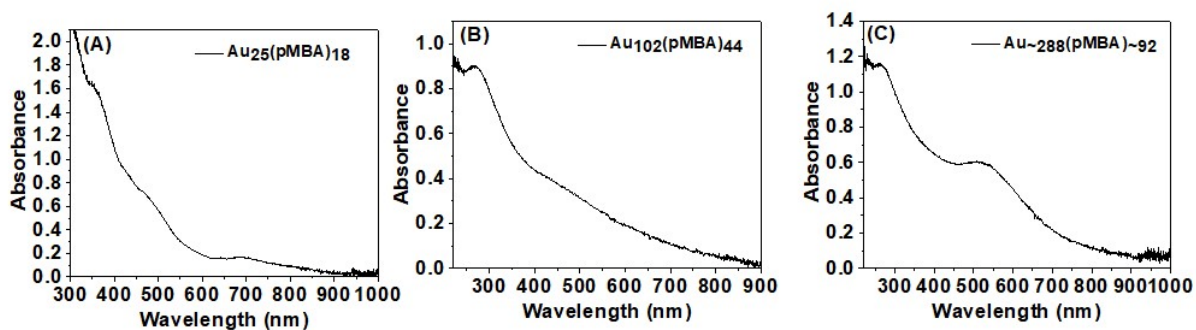


**Figure S3.** UV-vis absorption spectra of aqueous solutions of (A)  $\text{Au}_{25}(\text{pMBA})_{18}$ , (B)  $\text{Au}_{102}(\text{pMBA})_{44}$  and (C)  $\text{Au}_{\sim 288}(\text{pMBA})_{\sim 92}$  NCs.

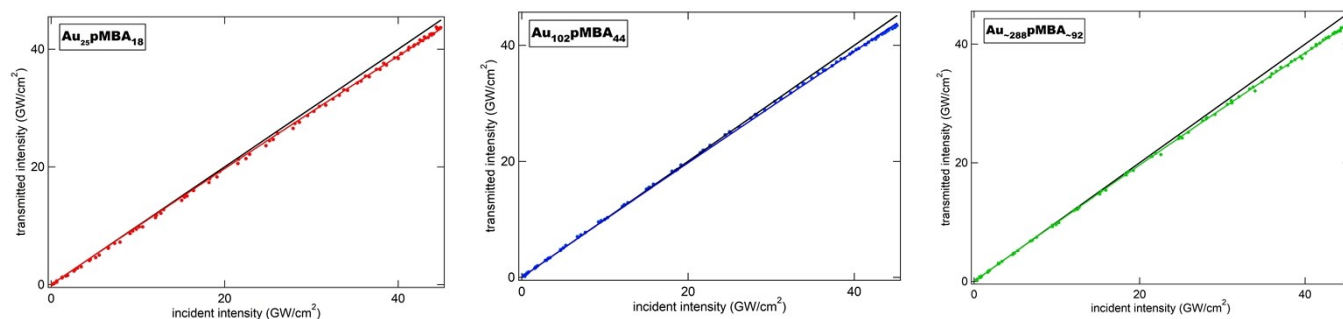


**Figure S4.** Transmitted intensity recorded at 808 nm (empty circles) with a cell of water, (filled circles) with the  $\text{Au}_{25}(\text{pMBA})_{18}$ ,  $\text{Au}_{102}(\text{pMBA})_{44}$  and  $\text{Au}_{\sim 288}(\text{pMBA})_{\sim 92}$  NCs solution. Solid lines are fit using nonlinear absorption.

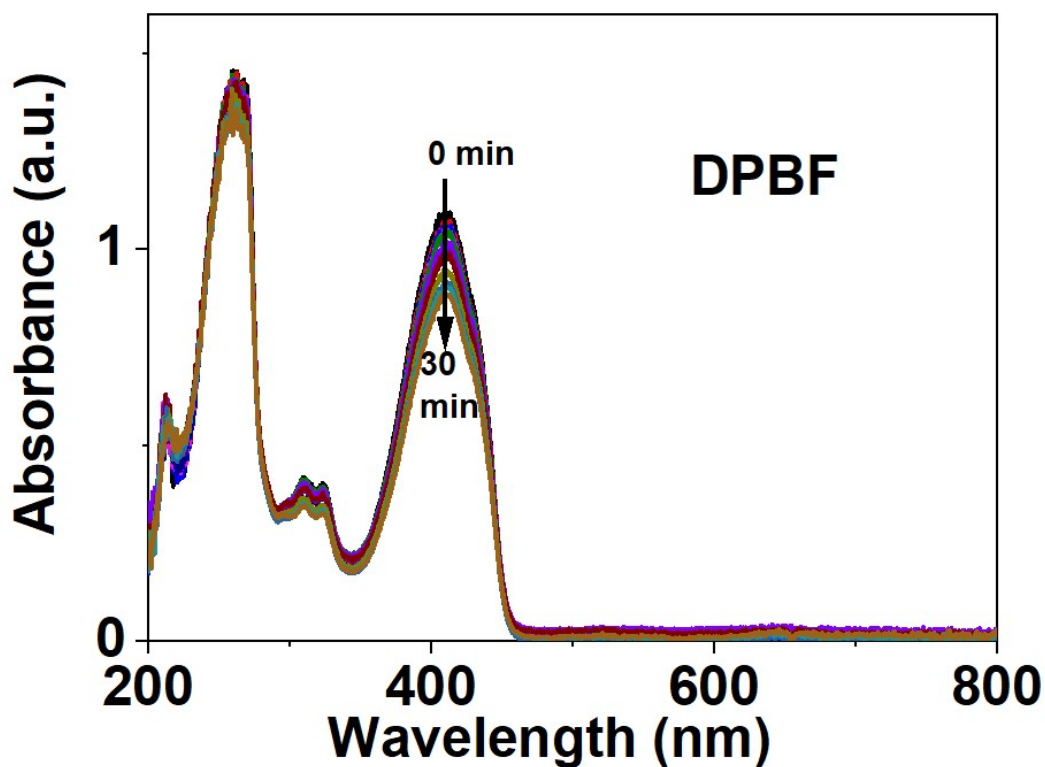


**Figure S5.** Absorption spectra of DPBF in water in the absence of NCs under irradiation with a 1W CW laser at 808 nm for 30 min.

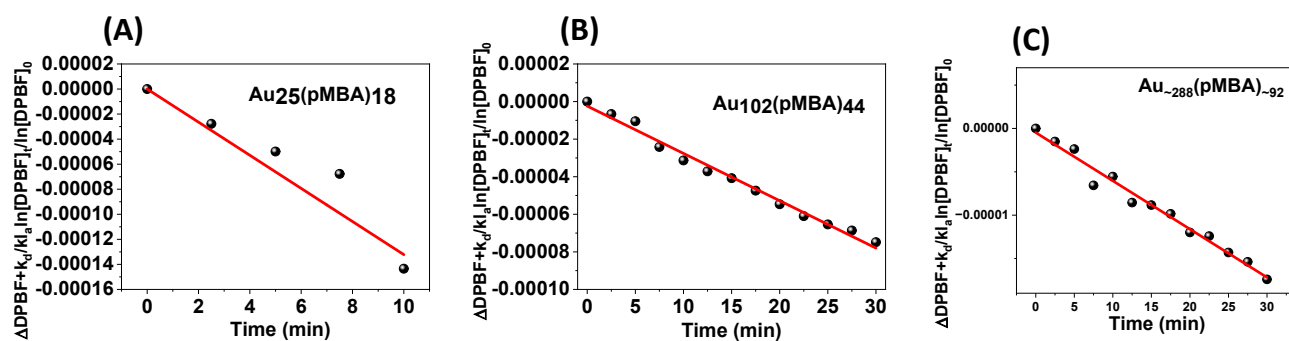


**Figure S6.** Comparison of the change in  $\Delta[\text{DPBF}] + k_d/k_a \ln([\text{DPBF}]_t/[\text{DPBF}]_0)$  with time for (A)  $\text{Au}_{25}(\text{pMBA})_{18}$ , (B)  $\text{Au}_{102}(\text{pMBA})_{44}$  and (C)  $\text{Au}_{-288}(\text{pMBA})_{-92}$  NCs under CW laser excitation at 808 nm.

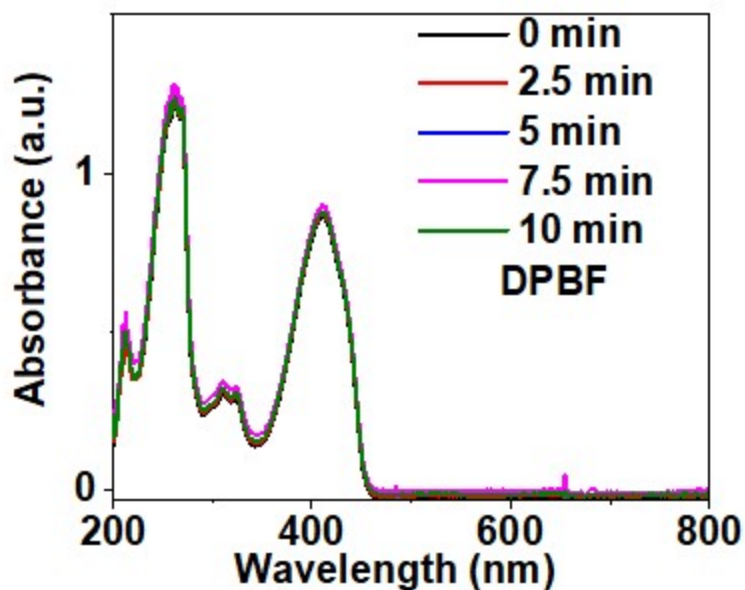


**Figure S7.** Absorption spectra of DPBF in water in the absence of NCs under irradiation with a 1W pulsed laser at 808 nm for 10 min.

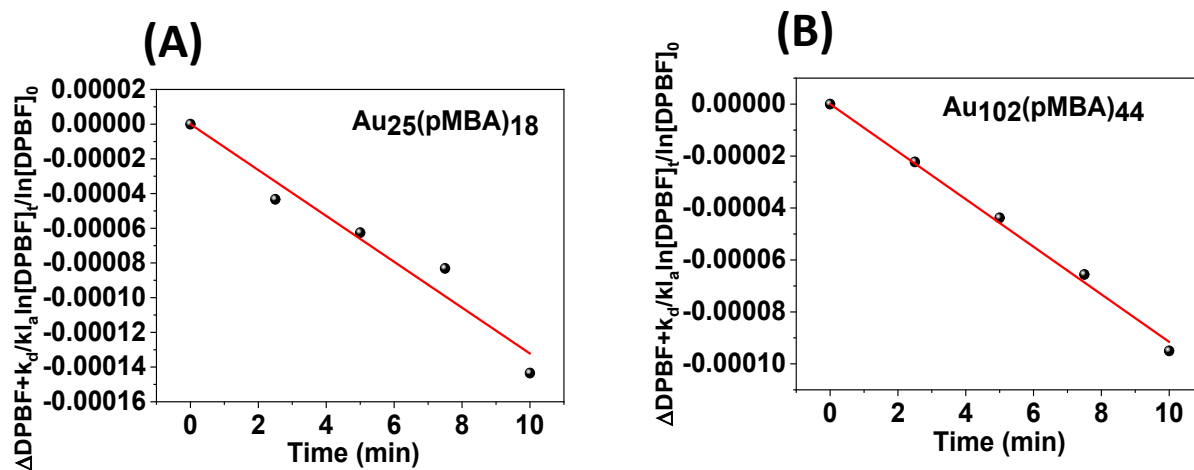


**Figure S8.** Comparison of the change in  $\Delta[\text{DPBF}] + k_d/k_a \ln([\text{DPBF}]_t/[\text{DPBF}]_0)$  with time for (A) Au<sub>25</sub>(pMBA)<sub>18</sub>, (B) Au<sub>102</sub>(pMBA)<sub>44</sub> NCs under pulsed laser excitation at 808 nm.

**References.**

1. Y. Zeng, C. Comby-Zerbino, B. Grimm-Lebsanft, M. Teubner, S. Reichenberger, R. Antoine, M. Rübhausen, S. Barcikowski, W. J. Parak and I. Chakraborty, *ACS Appl. Nano Mater.*, 2025, **8**, 13611-13619.
2. I. Russier-Antoine, F. Bertorelle, N. Calin, Ž. Sanader, M. Krstić, C. Comby-Zerbino, P. Dugourd, P. F. Brevet, V. Bonačić-Koutecký and R. Antoine, *Nanoscale*, 2017, **9**, 1221-1228.
3. D. K. Roper, W. Ahn and M. Hoepfner, *J. Phys. Chem. C*, 2007, **111**, 3636-3641.
4. R. Ho-Wu, S. H. Yau and T. Goodson, III, *The Journal of Physical Chemistry B*, 2017, **121**, 10073-10080.
5. D. M. Marin, S. Payerpaj, G. S. Collier, A. L. Ortiz, G. Singh, M. Jones and M. G. Walter, *Physical Chemistry Chemical Physics*, 2015, **17**, 29090-29096.
6. D. P. Damera, V. Krishna, V. V. K. Venuganti and A. Nag, *J Photochem Photobiol B*, 2021, **225**, 112335.
7. F. Wilkinson and J. G. Brummer, *Journal of Physical and Chemical Reference Data*, 1981, **10**, 809-999.
8. T. L. C. Figueiredo, R. A. W. Johnstone, A. M. P. S. Sørensen, D. Burget and P. Jacques, *Photochem. Photobiol.*, 1999, **69**, 517-528.